

Assessment of Neutral Voltages in Distribution Networks via Monte Carlo Simulation and Load Flow Independent Grounding Approximation

Henrique Pires CORRÊA, Flávio Henrique Teles VIEIRA, Lina Paola Garces NEGRETE
Universidade Federal de Goiás, 74605-010, Brazil
pires_correa@ufg.br

Abstract—The computation of neutral voltages in power systems via load flow algorithms and Monte Carlo simulation is a topic that is receiving increased attention in recent works due to growth in installed distributed generation. In this paper, a novel method is proposed for estimating neutral voltage probability density functions in terms of system grounding impedances and in the presence of stochastic distributed generation. The main advantage of the proposed method is that it does not require solving load flow for each set of possible grounding impedances. Instead, a single load flow is required for the entire set, whose results are then used for estimating neutral voltage as a function of grounding impedance via Y-bus inversion. A case study is carried out via simulation to validate the method. The obtained results suggest that the proposed method provides low estimation error and yields significant reduction in computational complexity with respect to the standard load flow-based method.

Index Terms—Monte Carlo methods, estimation, grounding, power distribution, distributed power generation.

I. INTRODUCTION

The rapid evolution of power distribution networks from traditional infrastructure and loading characteristics towards widespread usage of nonlinear loads and distributed renewable generation has sparked significant interest in evaluation of power quality indicators. Furthermore, greater attention has been dispensed to the analysis of factors that may cause the violation of quality criteria to which distribution utilities must comply.

Among the existing power quality indicators [1-4], this paper focuses on the assessment of neutral voltage. For an ideal power system, the magnitude of neutral voltage should be zero, either due to zero-resistance grounding or perfect phase balance and consequent lack of neutral current. In practice, such conditions cannot be achieved and measurable voltage can be detected between neutral and ground. Hence, neutral voltage is a function of load unbalance, neutral wire impedance and grounding impedances along the system.

In this context, two important reasons for assessing neutral voltage must be mentioned. Firstly, in most consumer properties neutral and earthing conductors are short-circuited at the main utility entrance panel and grounded at this point [5]; if the grounding resistance is not sufficiently low and system operation causes neutral voltage rise, all equipment to which the earthing conductor is bonded will be exposed to this voltage. A second reason is associated to the existence of communication equipment that use the earthing conductor for signal grounding purposes [6], which may suffer from disruption of communication

due to inadequate voltages present in the earthing conductor.

A small amount of works in the literature have proposed specific methods for computing neutral voltage in power systems. In general, the adopted approach consists in extending a given load flow algorithm to explicitly include neutral conductors and grounding impedances in its formulation. Such works present some disadvantages, such as: increment in admittance matrix order, requiring a load flow run for each set of grounding impedance values and not providing statistical results for neutral voltage. In this paper, a Monte Carlo-based approximate method is proposed that avoids such difficulties and provides histograms that can be used for the statistical assessment of neutral voltage.

A. Related Works

Previous works in the literature regarding neutral voltage computation are mostly limited to the extension of three-phase, three-wire load flow models and algorithms to encompass the neutral conductor and grounding. In [7], a procedure is established for using three-wire circuit component models derived in [8] in circuit simulation software to construct explicit-neutral simulation models. The authors in [9] extend the current-injection load flow method from [10] to include four-wire networks. In [11, 12], a forward-backward sweep method is proposed for solving four-wire power flow, being limited to radial distribution networks. In [13], an approximate and low complexity method for evaluating neutral voltage, without the usual requirements of extending the system admittance matrix and executing a new load flow run for each desired set of grounding impedance values is proposed.

A disadvantage of the above-mentioned works is that no means of statistically analyzing neutral voltage is provided. This analysis would be a desirable feature, since power quality is a function of typically stochastic factors such as load, allocation of distributed generation and renewable energy sources. In fact, multiple works assess other power quality indicators via Monte Carlo simulation. For example, in [14], weather forecast uncertainties are used as input to obtain output distributions for transmission conductor temperatures and assess probabilities of thermal limit violation. In [15], distributed generation units are randomly attributed to low-voltage feeder consumers for estimating bus voltage magnitude distributions. In [16, 17], the authors model probability distributions of photovoltaic generation and charging of plug-in electric vehicles to assess, respectively, voltage unbalance and transformer aging.

B. Contribution and Paper Organization

In this work, the method proposed in [13] is extended by incorporating the Monte Carlo method for computing neutral voltage distributions as functions of variable load and distributed generation. The original advantages of [13] shall contribute to reducing computational complexity associated to the Monte Carlo simulation.

This paper is organized as follows. In Section II, a discussion of neutral voltage computation via load flow is given. In Sections III and IV, the proposed combination of grounding approximation and Monte Carlo simulation is described. In Section V, the simulation of a case study using an IEEE test system is carried out to illustrate the method. In Section VI, conclusions regarding the results are drawn.

II. COMPUTATION OF NEUTRAL VOLTAGE

Neutral voltage magnitudes and angles, analogously to the corresponding phase quantities, are implicit functions of the nodal current injections in the power system buses. In a scenario where distributed generation is considered, such current injections are determined by the difference between currents corresponding to generated and load power, respectively. Due to the previously mentioned implicit functional relation, load flow methods must be applied in order to solve for all phase and neutral voltages.

In most instances of four-wire system load flow analysis, zero resistance neutral grounding is assumed. This allows the use of Kron reduction, which reduces the load flow problem to an equivalent three-wire system where effects of neutral impedance are directly incorporated in the phase mutual and self-impedances. However, assuming zero resistance grounding prevents the computation of neutral voltages. If they must be obtained, neutral conductors have to be explicitly represented in the admittance matrix.

Let a four-wire transmission line connect three-phase buses denoted by letters i and j . The explicit-neutral voltage drop equations are:

$$\begin{bmatrix} \Delta \hat{V}_{ij}^a \\ \Delta \hat{V}_{ij}^b \\ \Delta \hat{V}_{ij}^c \\ \Delta \hat{V}_{ij}^n \end{bmatrix} = \begin{bmatrix} \hat{V}_i^a - \hat{V}_j^a \\ \hat{V}_i^b - \hat{V}_j^b \\ \hat{V}_i^c - \hat{V}_j^c \\ \hat{V}_i^n - \hat{V}_j^n \end{bmatrix} = \underbrace{\begin{bmatrix} z_{aa} & z_{ab} & z_{ac} & z_{an} \\ z_{ba} & z_{bb} & z_{bc} & z_{bn} \\ z_{ca} & z_{cb} & z_{cc} & z_{cn} \\ z_{na} & z_{nb} & z_{nc} & z_{nn} \end{bmatrix}}_{\mathbf{Z}_{line}} \begin{bmatrix} \hat{I}_{ij}^a \\ \hat{I}_{ij}^b \\ \hat{I}_{ij}^c \\ \hat{I}_{ij}^n \end{bmatrix} \quad (1)$$

where, z_{rr} is the self-impedance of phase r , z_{rs} is the mutual impedance between phases r and s , \hat{V}_i^r is the voltage phasor of phase r in bus i and \hat{I}_{ij}^r is the current phasor flowing in phase r from i to j , with $r, s \in \{a, b, c, n\}$ and the letter n denotes *neutral conductor*.

Clearly, Kron reduction corresponds to setting $\Delta \hat{V}_{ij}^n = 0$.

Now, consider a four-wire power system with N buses and grounding impedances z_g^i , $i=1, 2, \dots, N$. The system admittance matrix \mathbf{Y} is of order $4N$ and given by 4×4 submatrices \mathbf{Y}_{ij} as $\mathbf{Y} = [\mathbf{Y}_{ij}]_{4N \times 4N}$, where $i, j = 1, 2, \dots, N$. These admittance submatrices are given by [18]:

$$\mathbf{Y}_{ii} = \mathbf{Y}_{ii}^{(sh)} + \sum_{j \in \Omega_i} \mathbf{Y}_{ij}^{(j)} \quad (2)$$

$$\mathbf{Y}_{ij} = -\mathbf{Y}_{ij}^{(i)} \quad (3)$$

where, the $\mathbf{Y}_{ij}^{(i)}$ are 4×4 primitive admittance matrices of the circuit element that connects buses i and j , Ω_i is the set of buses connected to bus i and $\mathbf{Y}_{ii}^{(sh)}$ is the primitive self-admittance matrix of bus i , which is given by [19]:

$$\mathbf{Y}_{ii}^{(sh)} = \mathbf{Y}_{ii}^{(c)} + \begin{bmatrix} 0 & 0 & 0 & 0 \\ 0 & 0 & 0 & 0 \\ 0 & 0 & 0 & 0 \\ 0 & 0 & 0 & z_g^i \end{bmatrix} \quad (4)$$

where, $\mathbf{Y}_{ii}^{(c)}$ encompasses shunt impedances corresponding to compensators and line capacitances. This decomposition shows that the admittance matrix, via its diagonal submatrices, is a function of system grounding impedances.

Suppose it is necessary to compute all \hat{V}_i^n as functions of the z_g^i defined in a domain $z_g^i \in \mathcal{Z} = \{z_g^{(1)}, z_g^{(2)}, \dots, z_g^{(M)}\}$, $M \in \mathbb{N}^*$. In order to evaluate neutral voltages for all possible combinations of z_g^i values, a total of M^N load flow problems have to be solved, which shows that the problem complexity grows exponentially with N .

Furthermore, if statistical assessment of \hat{V}_i^n is carried out considering variations in load and generation via Monte Carlo simulation, computational costs are further increased. In fact, if S load and generation profiles are sampled in the simulation, SM^N load flows will have to be carried out.

From such considerations, it is clear that employing statistical methods and four-wire load flow for assessing neutral voltages may lead to unacceptable execution times. Therefore, in this paper, a method that combines approximate neutral voltage computation and Monte Carlo simulation is proposed in order to significantly alleviate computational costs. As will be shown, the method reduces the number of required load flows from SM^N to S .

III. GROUNDING IMPEDANCE APPROXIMATION

A. Overview of the Approximation Method

When zero resistance grounding is assumed, Kron reduction may be applied to (1) for reducing \mathbf{Z}_{line} to a 3×3 matrix involving only phase voltages and currents. Furthermore, the last row from (1) can be used to obtain the following estimation for the neutral current phasor:

$$\hat{I}_{ij}^n \approx -\frac{z_{na} \hat{I}_{ij}^a + z_{nb} \hat{I}_{ij}^b + z_{nc} \hat{I}_{ij}^c}{z_{nn}} \quad (5)$$

Hence, by solving load flow for the Kron-reduced $3N \times 3N$ system admittance matrix and applying (5), neutral current can be computed (but not neutral voltage, which is assumed at zero potential). Now, it can be argued that, for usual four-wire power systems, applying (5) is an adequate approximation even if perfect grounding is not assumed.

Even if $z_g^i \neq 0$, the grounding impedances in four-wire systems are sufficiently low to make the neutral voltage significantly closer to zero (in magnitude) than other system magnitudes, such as phase currents and voltages. Manipulating the last equation in (1), it can be seen that:

$$\hat{I}_{ij}^n = \frac{\Delta \hat{V}_{ij}^n - z_{na} \hat{I}_{ij}^a - z_{nb} \hat{I}_{ij}^b - z_{nc} \hat{I}_{ij}^c}{z_{nn}} \quad (6)$$

where, due to the small neutral voltage magnitudes, $\Delta \hat{V}_{ij}^n$ is dominated by the other terms in the numerator. In this sense, by considering $|\Delta \hat{V}_{ij}^n| \approx 0$, it is clear that (6) reduces to the Kron reduction equation given by (5).

In [13], it is shown that an equivalent circuit based on (5) can be constructed for estimating all \hat{V}_i^n in the system. The main features of the equivalent circuit are the following:

1. Each bus neutral voltage is modeled by a single node;
2. Each \hat{I}_{ij}^n estimated using (5) is modeled by a current source connected between ground and node i , with its direction adjusted according to the upstream or downstream direction of current with respect to the phase-frame representation of the system;
3. The transmission line connecting buses i and j is modeled by its neutral self-impedance z_{nn} connected between the corresponding nodes;
4. Each z_g^i is connected from its node to ground.

By constructing the equivalent circuit for a given set of \hat{I}_{ij}^n estimated via three-wire load flow and (5), neutral voltages can be estimated for arbitrary values of z_g^i by solving the equivalent circuit using Y-bus inversion. Hence, for the impedance domain \mathcal{Z} defined in Section II, a total of one load flow and M^N iterations of Y-bus inversion are required. This is a favorable scenario in comparison with the execution of M^N four-wire load flows, since:

1. Y-bus inversion is linear and consists in one matrix inversion, whereas load flow is nonlinear and may require multiple Jacobian inversions;
2. Four-wire load flow may lead to a poorly conditioned Jacobian, due to the linear dependence between phase and neutral currents in each bus.

In Section IV, we shall propose incorporation of this approximate method into a Monte Carlo simulation, which will enable the statistical assessment of neutral voltage. Assuming S random samples are used, it is clear that the overall procedure requires S load flows and SM^N inversions of the equivalent circuit Y-bus matrix. In Table I, comparison between computational requirements is shown.

TABLE I. COMPARISON OF COMPUTATIONAL REQUIREMENTS

Method	# Load Flows	# Y-bus Inversions
Four-wire load flow	SM^N	0
Proposed	S	SM^N

It is of greater interest to compare computational complexities in terms of *big-O* notation, instead of solely computing the required number of load flow and Y-bus inversions. To achieve this, it is assumed that standard Gaussian elimination is used for matrix inversion, which has an arithmetic complexity of $O(N^3)$ [20].

Assume that solving each load flow requires, on average, a total of P matrix inversions. In this sense, it is clear that, assuming $O(N^3)$ complexity for matrix inversion, the method based on standard four-wire load flow has a

complexity of $O(SN^3PM^N)$. Proceeding in a similar manner, the proposed method achieves a computational complexity $O(SN^3(P+M^N))$, which is advantageous in comparison to the standard method. This comparison in terms of complexity is summarized in Table II.

TABLE II. COMPARISON OF COMPUTATIONAL COMPLEXITIES

Method	Complexity
Four-wire load flow	$O(SN^3PM^N)$
Proposed	$O(SN^3(P+M^N))$

B. Discussion of Approximation Error

We now discuss the error yielded by the base approximation method [13] and show why it is valid for low grounding impedances, as previously mentioned.

Consider a transmission line connecting buses i and j , as in Section II. The circuit obtained via application of items 1-4 from Section III-A is shown in Figure 1.

At first, note that the *injection* current in each neutral node is taken as \hat{I}_{ij}^n , which is the neutral *line* current. Now, let \hat{I}_i^n denote the true injection current in neutral node i . It will now be shown that substituting \hat{I}_{ij}^n for \hat{I}_i^n provides good accuracy for low z_g^i . Considering, at first, a zero resistance grounding scenario, it can be expected that the neutral conductor will present sufficient impedance with respect to ground so that $|\hat{I}_{ij}^n| < |\hat{I}_i^n|$ for $z_i^g = z_j^g = 0$.

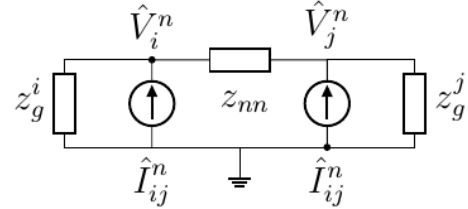


Figure 1. Equivalent neutral circuit for transmission line, according to [13]

As $z_g^{ij} = z_g^i + z_g^j$ increases, $|\hat{I}_{ij}^n|$ increases and $|\hat{I}_i^n|$ decreases. Now, for a high z_{ij} , it can be expected that $|\hat{I}_i^n| \rightarrow 0$ and, therefore, there will be a sufficiently low value of z_g^{ij} , denoted by $z_{g_a}^{ij}$, for which $|\hat{I}_{ij}^n(z_{g_a}^{ij})| = |\hat{I}_i^n(z_{g_a}^{ij})|$. This fact is illustrated in Figure 2, in which \mathcal{Z}_a denotes the neighborhood of $z_{g_a}^{ij}$ where using $|\hat{I}_i^n| \approx |\hat{I}_{ij}^n|$ is an acceptable approximation.

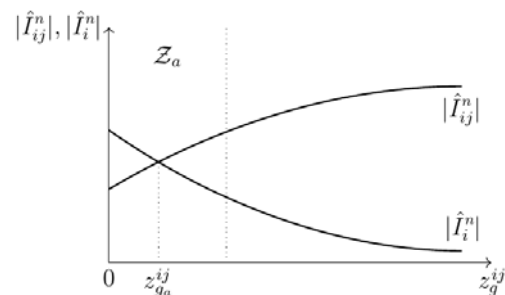


Figure 2. Neighborhood \mathcal{Z}_a of $z_{g_a}^{ij}$ in which $|\hat{I}_i^n| \approx |\hat{I}_{ij}^n|$.

Now that $|\hat{I}_i^n| \approx |\hat{I}_{ij}^n|$ has been established in \mathcal{Z}_a , the behavior of \hat{V}_i^n as computed from the circuit of Figure 1 is analyzed. Solving such circuit for \hat{V}_i^n , we obtain:

$$\hat{V}_i^n = \frac{z_{nm} + z_g^i}{z_{nm} + z_g^i + z_g^j} \cdot z_g^i \hat{I}_{ij}^n + \frac{z_g^i}{z_{nm} + z_g^i + z_g^j} \cdot z_g^j \hat{I}_{ij}^n \quad (7)$$

where, for $z_i^g, z_j^g \rightarrow 0$, we obtain $\hat{V}_i^n = z_g^i \hat{I}_{ij}^n \approx z_g^i \hat{I}_i^n$, which is consistent with the computation of neutral voltage through injection current. It can be seen in (7) that, for small grounding impedances, decreases in z_g^i tend to reduce $|\hat{V}_i^n|$ and variations in z_g^j have small influence over $|\hat{V}_i^n|$; this is also coherent with expected behavior for small z_g^i and z_g^j .

IV. MONTE CARLO SIMULATION

To obtain neutral voltage probability distributions, we take load and distributed generation in each bus as stochastic and model them as discrete random variables. To draw samples from the random variables, the inverse transform method [21, 22] is used, which is now described. Let X be a discrete random variable with domain $\mathcal{X} = \{x_1, x_2, \dots, x_K\}$, $K \in \mathbb{N}^*$, and probabilities $P(X = x_i) = p_i$. For sampling X , first draw a random sample u from the continuous uniform distribution $U(0,1)$. Then, verify for which positive integer l the following inequalities are satisfied:

$$F(x_{l-1}) = \sum_{i=1}^{l-1} p_i < u \leq \sum_{i=1}^l p_i = F(x_l) \quad (8)$$

where $F(x)$ is the cumulative distribution of X . Given the l for which (8) is satisfied, the sample $X = x_l$ is drawn.

Denote the joint samples drawn for load and distributed generation by s_j , $j = 1, 2, \dots, S$. For each s_j , one three-wire load flow problem and M^N equivalent circuit Y-bus inversions are computed, as discussed in Section III. The output consists in neutral voltage phasors for each possible combination of grounding impedances, i.e. $\hat{V}_i^n(\mathbf{z}_g, s_j)$, with $i = 1, 2, \dots, N$ and $\mathbf{z}_g = [z_g^1 \ z_g^2 \ \dots \ z_g^M]^T$, $z_g^i \in \mathcal{Z}$. In what follows, we focus solely on the corresponding neutral voltage magnitudes, which we denote by $V_i^n(\mathbf{z}_g, s_j)$.

The S values of $V_i^n(\mathbf{z}_g, s_j)$ for a given \mathbf{z}_g can be used to compute a voltage magnitude distribution corresponding to \mathbf{z}_g , i.e. a distribution for $V_i^n(\mathbf{z}_g)$. To accomplish this, a bin size ΔV must be chosen for partitioning the interval $(0, \max_j V_i^n(\mathbf{z}_g, s_j)]$ in disjoint subintervals:

$$(0, \max_j V_i^n(\mathbf{z}_g, s_j)] = \bigcup_{r=1}^L ((r-1)\Delta V, r\Delta V] \quad (9)$$

where, $L = \max_j V_i^n(\mathbf{z}_g, s_j) / \Delta V$. For the obtained subintervals, the distribution for $V_i^n(\mathbf{z}_g)$ can be computed by means of relative frequencies:

$$\hat{f}_{V_i^n(\mathbf{z}_g)}(r) = \frac{\#\{V_i^n(\mathbf{z}_g, s_j) | (r-1)\Delta V < V_i^n(\mathbf{z}_g, s_j) \leq r\Delta V\}}{S} \quad (10)$$

where, the symbol $\#$ denotes the number of elements in a set and the index $r = 1, 2, \dots, L$. For each subinterval, the mean of its extremes is considered as the representative value. Hence, for the subinterval $((r-1)\Delta V, r\Delta V]$, this representative value is equal to $(2r-1) \cdot \Delta V / 2$ and thus:

$$\hat{f}_{V_i^n(\mathbf{z}_g)}(r) = \hat{P} \left\{ V_i^n(\mathbf{z}_g, s_j) = \frac{2r-1}{2} \Delta V \right\} \quad (11)$$

By running the required S load flows and SM^N Y-bus inversions, the distributions $\hat{f}_{V_i^n(\mathbf{z}_g)}$ are obtained for all $i = 1, 2, \dots, N$ and $\mathbf{z}_g \in \mathcal{Z}^M$. The pseudocode corresponding to the proposed method is given in Figure 3.

Algorithm Method for statistical assessment of neutral voltage

Input: $\hat{I}_{ij}^n, z_{nm}; \mathcal{Z}; S; \Delta V; i, j = 1, 2, \dots, N$.

```

1: for  $1 \leq s \leq S$  do
2:   for  $1 \leq i \leq N$  do
3:     for  $\mathbf{z}_g \in \mathcal{Z}^M$  do
4:       Construct and solve equivalent circuit [13].
5:     end for
6:     return  $V_i^n(\mathbf{z}_g, s_j); \mathbf{z}_g \in \mathcal{Z}^M$ .
7:   end for
8:   Compute distributions via (9)–(11).
9: end for
10: return  $\hat{f}_{V_i^n(\mathbf{z}_g)}; i = 1, 2, \dots, N$  and  $\mathbf{z}_g \in \mathcal{Z}^M$ .

```

Figure 3. Pseudocode of the proposed method

V. CASE STUDY

A. Test System Description

To illustrate the proposed method, a case study is carried out on the standard IEEE 4-bus test feeder in its unbalanced load and step-down delta-wye transformer configuration [23]. This system was selected due to its small number of four-wire buses, which enables an easier visualization of the statistical results yielded by the proposed method.

The test system consists in a grounded wye-connected unbalanced load (bus 4) fed by the grounded wye secondary of a step-down transformer (bus 3) through a 762-meter four-wire transmission line. The transformer primary is delta-connected (bus 2) and is fed by an infinite bus (bus 1) by means of a 610-meter three-wire transmission line. High and low voltage nominal values are, respectively, 12.47 kV and 4.16 kV. Documentation of the test feeder impedances and reference load flow results are discussed in [23].

This feeder configuration was selected due to it being, among the ones available for the 4-bus test feeder [23], most representative of typical distribution systems. In fact, the 12.47 kV line assumes the role of a high-voltage line which supplies a distribution transformer, whereas the four-wire 4.16 kV line represents a low-voltage, neutral-equipped line that feeds a three-phase consumer load.

Random load and distributed generation in the four-wire feeder are simulated as follows. In the original system, a constant and unbalanced load is located in bus 4; let $[P_4^\phi]_o$ and $[Q_4^\phi]_o$ denote original active and reactive powers in phase $\phi \in \{a, b, c\}$ of bus 4, respectively. To simulate load uncertainties, these power values are multiplied by independent and identically distributed (i.i.d.) samples of the random variable $X_{load} = U'(-30, 30) / 100$, where U' is the

discrete uniform distribution. In other words, active and reactive loads may vary up to 30% below or above the original system values, in 1% increments:

$$P_4^\phi = \frac{[P_4^\phi]_o}{100} \cdot U'(-30,30) \quad (12)$$

$$Q_4^\phi = \frac{[Q_4^\phi]_o}{100} \cdot U'(-30,30) \quad (13)$$

It is assumed that distributed generation may be allocated to any of the system buses. To emulate this, i.i.d. samples of a random variable $X_{allocation} \sim \text{Bernoulli}(0.5)$ are associated to each bus in each iteration of the Monte Carlo simulation. If $x_{allocation} = 1$ for a given bus, distributed generation is allocated to it. We consider that distributed generation units operate at unit power factor and the generated active power of each bus and phase, $P_{G,i}^\phi$, $i = 1, 2, 3, 4$, is modeled as:

$$P_{G,i}^\phi = \frac{[P_4^\phi]_o}{100} \cdot U'(0,100) \quad (14)$$

which means that generated power in each phase is assumed to be uniformly distributed between zero and 100% of the nominal load of such phase.

The model used for simulating distributed generation is illustrated in Figure 4. It should be noted that arbitrary distributions can be selected for modeling load and distributed generation; in this work, an uniform distribution was chosen in order to simplify the case study.

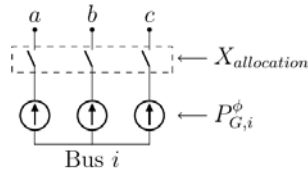


Figure 4. Model used for simulating distributed generation

In the 4-bus system, the neutral voltages to be computed are \hat{V}_3^n and \hat{V}_4^n , since the remaining buses are located in the delta side. For the Monte Carlo simulation, values of $S = 5000$, $\Delta V = 0.1 \text{ V}$ and the grounding impedance domain $\mathcal{Z} = \{0.1 \cdot i \Omega; i = 1, \dots, 4\}$ were specified. Since there are two neutral nodes, the analysis of grounding impedance must be carried out over \mathcal{Z}^2 , with $\mathbf{z}_g = [z_g^3 \ z_g^4]^T$.

B. Simulation Results

To facilitate visualization of simulation results, the following procedures are adopted for plotting the obtained distributions: (a) only distributions of V_3^n are plotted due to symmetry of Bus 4 with respect to Bus 3, in terms of neutral wire and grounding, (b) distributions for fixed z_g^3 and varying z_g^4 are plotted together for assessing the effect of remote grounding (z_g^4) in a local node (V_3^n), and (c) plots with fixed z_g^4 and varying z_g^3 are constructed for analyzing the effect of local grounding (z_g^3) in the local node.

The obtained results are given in Tables III, IV and Figures 5 to 12. In general, the results behave as expected in terms of neutral voltage as a function of grounding. The following are interesting features of the results:

1. For fixed z_g^3 , variations in z_g^4 do not cause large changes in the average of V_3^n ; the main noticeable effect of varying remote grounding consists in the variation of neutral voltage variance;
2. For fixed remote grounding, the influence of z_g^3 over the neutral voltage distribution is significant, both in terms of average and variance. This shows that, as could be expected, neutral voltage is determined to a large degree by local grounding;
3. In the worst-case scenario $z_g^3 = z_g^4 = 0.4 \Omega$, values of V_3^n above 200 V were obtained. Hence, this simple case study shows that inadequate grounding impedance may expose users to dangerous voltages.

TABLE III. OBTAINED AVERAGES OF V_3^n (V)

z_g^3 (\Omega) \backslash z_g^4 (\Omega)	0.1	0.2	0.3	0.4
0.1	22.2	23.7	25.4	27.0
0.2	43.9	46.9	50.1	53.3
0.3	62.6	66.8	71.5	76.2
0.4	78.6	84.0	90.0	96.2

TABLE IV. OBTAINED VARIANCES OF V_3^n (V²)

z_g^3 (\Omega) \backslash z_g^4 (\Omega)	0.1	0.2	0.3	0.4
0.1	23.6	27.0	31.0	35.0
0.2	92.3	105.0	120.0	136.0
0.3	188.0	214.0	245.0	279.0
0.4	296.0	338.0	389.0	443.0

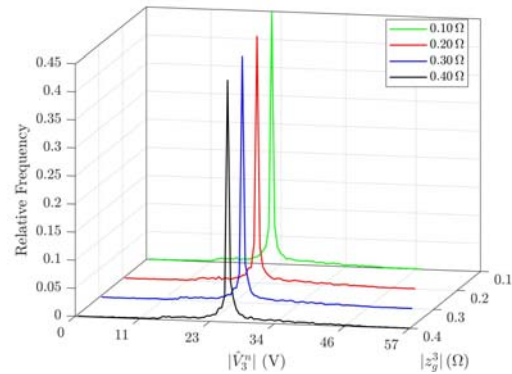


Figure 5. Distribution plots for fixed $z_g^3 = 0.1 \Omega$ and varying z_g^4

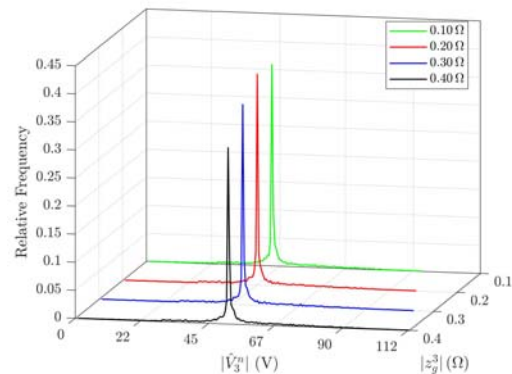


Figure 6. Distribution plots for fixed $z_g^3 = 0.2 \Omega$ and varying z_g^4

To further illustrate the main objective of the proposed method, all obtained distributions were used for estimating probability density functions for $V_3^n(\mathbf{z}_g)$, $\mathbf{z}_g \in \mathcal{Z}^2$.

$$\hat{\mu} = \text{median}\{V_3^n(\mathbf{z}_g, s_i), i = 1, 2, \dots, S\} \quad (16)$$

$$\hat{b} = \frac{1}{S} \sum_{i=1}^S |V_3^n(\mathbf{z}_g, s_i) - \hat{\mu}| \quad (17)$$

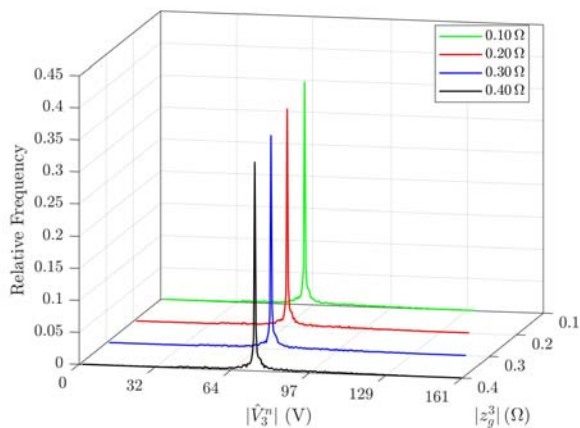


Figure 7. Distribution plots for fixed $z_g^3 = 0.3 \Omega$ and varying z_g^4

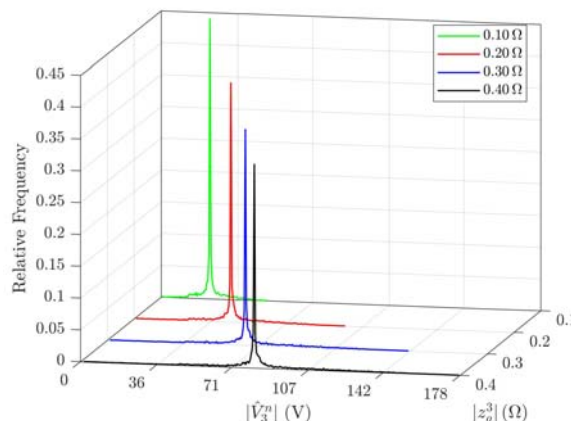


Figure 10. Distribution plots for fixed $z_g^4 = 0.2 \Omega$ and varying z_g^3

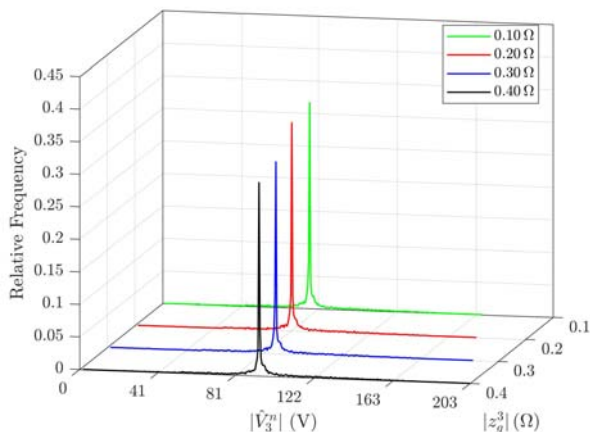


Figure 8. Distribution plots for fixed $z_g^3 = 0.4 \Omega$ and varying z_g^4

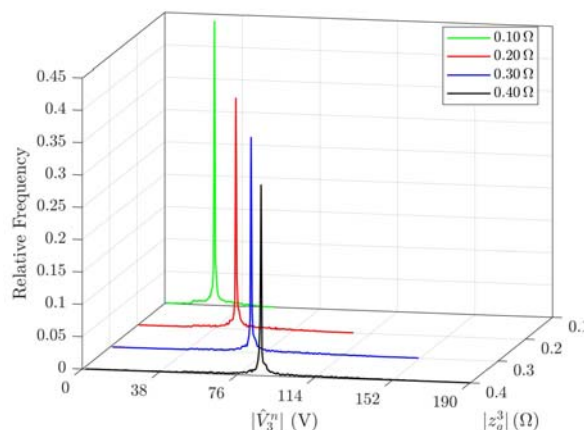


Figure 11. Distribution plots for fixed $z_g^4 = 0.3 \Omega$ and varying z_g^3

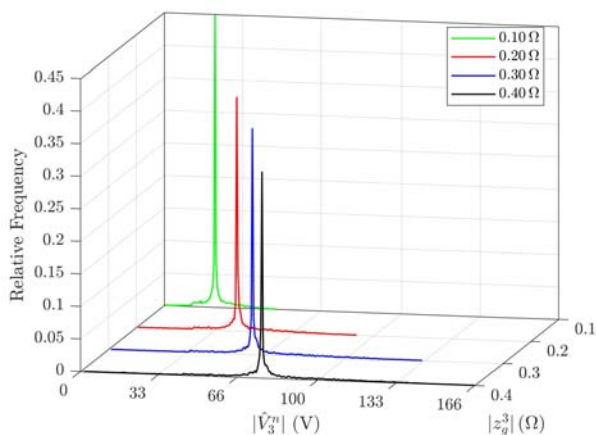


Figure 9. Distribution plots for fixed $z_g^4 = 0.1 \Omega$ and varying z_g^3

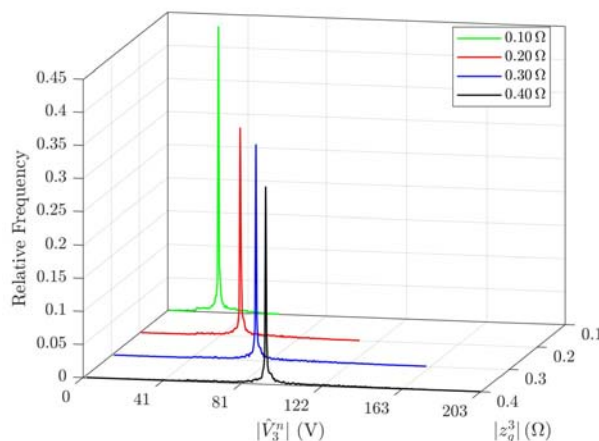


Figure 12. Distribution plots for fixed $z_g^4 = 0.4 \Omega$ and varying z_g^3

To achieve this, maximum likelihood estimation was used with the Laplace distribution:

$$f_{V_3^n(\mathbf{z}_g)}(v) = \frac{1}{2b} \cdot \exp\left(-\frac{|v - \mu|}{b}\right) \quad (15)$$

where, μ and b are the Laplace parameters. This distribution was selected due to the sharp unimodal form of the distributions obtained via Monte Carlo simulation. The maximum likelihood estimators are:

The obtained maximum likelihood parameters are given in Tables V and VI. To illustrate the results, Monte Carlo probability/cumulative mass functions (PMF/CMF) are compared to the estimated Laplace probability density and cumulative distribution functions (PDF and CDF) in Figures 13 and 14, for the cases $z_g^3 = z_g^4$, $z \in \mathcal{Z}$. In what follows, we comment the comparison under consideration.

The obtained results show that the maximum likelihood fitting of the Laplace distribution was able to provide acceptable accuracy with respect to the obtained discrete Monte Carlo distribution. It should be noted that any distribution could have been considered, as was the case for the distributed generation power and allocation models. This example was restricted to a single estimated distribution as a means of simplifying the analysis.

It is of interest to observe that the Monte Carlo PMF is narrower with respect to the corresponding Laplace PDF. However, this does not imply a bad fit via maximum likelihood estimation. Instead, this is a consequence of the Laplace PDF being continuous, whereas the Monte Carlo PMF is a discrete distribution. In this sense, the quality of fit is better represented by the CMF/CDF comparison.

TABLE V. ESTIMATED VALUES FOR LAPLACE PARAMETER μ (V)

$z_g^3(\Omega) \backslash z_g^4(\Omega)$	0.1	0.2	0.3	0.4
0.1	21.6	23.1	24.8	26.3
0.2	42.7	45.6	48.8	52.0
0.3	61.0	65.1	69.7	74.3
0.4	76.6	81.8	87.7	93.7

TABLE VI. ESTIMATED VALUES FOR LAPLACE PARAMETER b (V)

$z_g^3(\Omega) \backslash z_g^4(\Omega)$	0.1	0.2	0.3	0.4
0.1	2.50	2.68	2.87	3.05
0.2	4.95	5.29	5.66	6.02
0.3	7.06	7.54	8.07	8.60
0.4	8.87	9.47	10.20	10.90

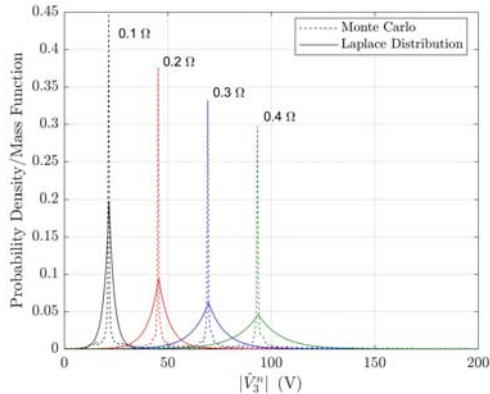


Figure 13. Comparison between Monte Carlo PMF and Laplace PDF

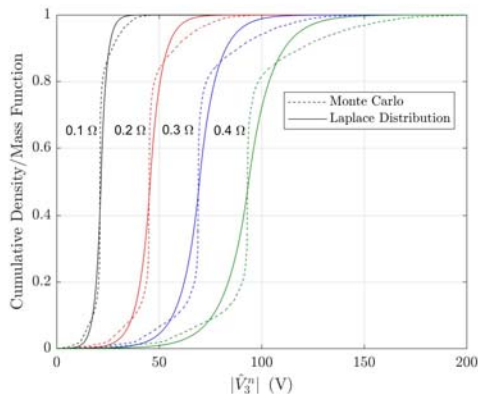


Figure 14. Comparison between Monte Carlo CMF and Laplace CDF

C. Analysis of Error and Execution Time

To validate the computational complexity and accuracy yielded by the proposed method, the case study considered in Section V-B was also solved by means of the standard load flow-based approach, for the sake of comparison. For computing neutral voltages via the standard method, Monte Carlo load flow was executed with the previously used parameters (i.e., $S = 5000$, $\Delta V = 0.1$ V) for each $\mathbf{z}_g \in \mathcal{Z}^2$.

In order to compare both methods, the following results were considered: execution time of both methods and the root mean square error (RMSE) of the Monte Carlo distribution for V_n^3 obtained via the proposed method, with respect to the one yielded by load flow computations. The execution times of both methods are detailed in Table VII, where *processing time* refers to the auxiliary computations, i.e. Y-bus inversion, required by the proposed method for estimating neutral voltage. In Table VIII, distribution RMSE is given (in volts) for each impedance vector.

Regarding execution times, it is important to mention that all simulation code was implemented in the MATLAB R2019a software, which in turn was executed in a dual-core 2.7GHz laptop computer.

TABLE VII. COMPARISON OF EXECUTION TIMES

Method	Execution time (s)		
	Load Flow	Processing	Total
Four-wire load flow	88.86	-	88.86
Proposed	5.11	0.11	5.22

TABLE VIII. DISTRIBUTION ROOT MEAN SQUARE ERRORS (V)

$z_g^3(\Omega) \backslash z_g^4(\Omega)$	0.1	0.2	0.3	0.4
0.1	4.24	3.82	3.43	0.55
0.2	1.37	7.38	3.30	1.63
0.3	8.60	6.31	1.59	3.23
0.4	10.25	7.64	3.80	2.72

From the data given in Table VII, it is clear that the proposed method yielded significant reduction in execution time with respect to standard computations. The results also validate the previous assertion that Y-bus inversion (processing time in Table VII) is faster than load flow and, for this reason, yields smaller execution times.

It is of interest to compare such results with the computational complexity analysis from Section III-A. By subtracting the complexity associated to the proposed method from the standard method complexity, a difference of $O(SN^3((P-1)M^N - P))$ is obtained. Considering that the number M^N is usually much larger than P , this can be approximated by $O(SN^3(P-1)M^N)$. By recalling that the original complexity is $O(SN^3PM^N)$, it is seen that the complexity reduction amounts to a factor of $(P-1)/P$.

As an approximation, by averaging over the number of load flow matrix inversions P throughout the simulations, a mean value of $\bar{P} = 5.98$ is obtained, which produces an average reduction factor $(\bar{P}-1)/\bar{P} \approx 85.67\%$. Despite this being an approximate factor, it agrees reasonably with the

obtained results, which have shown even better performance with a reduction of 94.12% in total execution time.

The data from Table VIII suggest that reasonable precision is attained with the proposed method. In fact, only a single distribution (i.e. $z_g^3 = 0.4 \Omega$ and $z_g^4 = 0.1 \Omega$) presented an associated RMSE superior to 10 V. It should be noted that assessment of neutral voltage for practical purposes, i.e. safety and grounding potential analysis, does not require highly precise computations. Hence, the combination of reasonable RMSE and substantial reduction of execution time shows that the proposed method is adequate for applications in which fast computation of an estimate for neutral voltage distribution is required.

VI. CONCLUSION

An approximate method for carrying out the statistical evaluation of neutral voltage in power systems has been proposed. The advantages of the proposed method are the reduction in computational complexity, with respect to standard load flow-based methods, and the output of estimated distributions for neutral voltage magnitude, which allow the computation of probabilities and carrying out statistical studies. Validation of the proposed method was achieved through a case study, whose results were shown to be coherent to expected neutral voltage behavior and, when compared to standard load flow-based computations, yielded reasonable estimation error and significant reduction in execution time. Such characteristics suggest that the proposed method is an adequate tool for practice-oriented, approximate assessment of neutral voltage probability distributions in the presence of renewable generation.

REFERENCES

- [1] D. Graovac, V. Katic and A. Rufer, "Power quality compensation using universal power quality conditioning system," *IEEE Power Engineering Review*, 2000, 20, (12), pp. 58–60. doi:10.1109/39.890381
- [2] W.E. Kazibwe, R.J. Ringlee, G.W. Woodzell and H.M. Sendaula, "Power quality: A review," *IEEE Computer Applications in Power*, 1990, 3, (1), pp. 39–42. doi:10.1109/67.53204
- [3] H.M.S.C Herath, V.J. Gosbell, and S. Perera, "Power quality (PQ) survey reporting: Discrete disturbance limits," *IEEE Transactions on Power Delivery*, 2005, 20, (2), pp. 851–858. doi:10.1109/TPWRD.2005.844257
- [4] F. Nejabatkhah, Y.W. Li and H. Tian, "Power quality control of smart hybrid AC/DC microgrids: An overview," *IEEE Access*, 2019, 7, pp. 52295–52318. doi:10.1109/ACCESS.2019.2912376
- [5] K. Bhatia, P.B. Darji and H.R. Jariwala, "Safety analysis of TN-S and TN-C-S earthing system," 2018 IEEE International Conference on Environment and Electrical Engineering and 2018 IEEE Industrial and Commercial Power Systems Europe (EEEIC/I CPS Europe), 2018, pp. 1–6. doi:10.1109/EEEIC.2018.8493856
- [6] R.B. Standler, "Protection of electronic circuits from overvoltages," *Electrical Engineering Series*. Dover Publications, 2002.
- [7] T.H. Chen and W.C. Yang, "Analysis of multi-grounded four-wire distribution systems considering the neutral grounding," *IEEE Transactions on Power Delivery*, 2001, 16, (4), pp. 710–717. doi:10.1109/61.956760
- [8] T. Chen, M. Chen, T. Inoue, P. Kotas, and E.A. Chebli, "Three-phase cogenerator and transformer models for distribution system analysis," *IEEE Transactions on Power Delivery*, 1991, 6, (4), pp. 1671–1681. doi:10.1109/61.97706
- [9] D.R.R. Penido, L.R. de Araujo, S. Carneiro, J.L.R. Pereira and P.A.N. Garcia, "Three-phase power flow based on four-conductor current injection method for unbalanced distribution networks," *IEEE Transactions on Power Systems*, 2008, 23, (2), pp. 494–503. doi:10.1109/TPWRS.2008.919423
- [10] V.M. da Costa, M.L. de Oliveira and M.R. Guedes, "Developments in the analysis of unbalanced three-phase power flow solutions," *International Journal of Electrical Power & Energy Systems*, 2007, 29, (2), pp. 175 – 182. doi:10.1016/j.ijepes.2006.06.005
- [11] R.M. Ciric, L.F. Ochoa and A. Padilha, "Power flow in distribution networks with earth return," *International Journal of Electrical Power & Energy Systems*, 2004, 26, (5), pp. 373 – 380. doi:10.1016/j.ijepes.2003.11.006
- [12] R.M. Ciric, A.P. Feltrin and L.F. Ochoa, "Power flow in four-wire distribution networks - General approach," *IEEE Transactions on Power Systems*, 2003, 18, (4), pp. 1283–1290. doi:10.1109/TPWRS.2003.818597
- [13] H.P. Corrêa and F.H.T. Vieira, "Load flow independent method for estimating neutral voltage in three-phase power systems," *Energies*, 2019, 12, (17). doi:10.3390/en12112039
- [14] D. Poli, P. Pelacchi, G. Lutzemberger, T.B. Scirocco, F. Bassi and G. Bruno, "The possible impact of weather uncertainty on the dynamic thermal rating of transmission power Lines: A Monte Carlo error-based approach," *Electric Power Systems Research*, 2019, 170, pp. 338 – 347. doi:10.1016/j.epr.2019.01.026
- [15] C.T. Gaunt, E. Namanya and R. Herman, "Voltage modelling of LV feeders with dispersed generation: Limits of penetration of randomly connected photovoltaic generation," *Electric Power Systems Research*, 2017, 143, pp. 1 – 6. doi:10.1016/j.epr.2016.08.042
- [16] M.K. Gray and W.G. Morsi, "Probabilistic quantification of voltage unbalance and neutral current in secondary distribution systems due to plug-in battery electric vehicles charging," *Electric Power Systems Research*, 2016, 133, pp. 249 – 256. doi:10.1016/j.epr.2015.12.022
- [17] M.K. Gray and W.G. Morsi, "On the impact of single-phase plug-in electric vehicles charging and rooftop solar photovoltaic on distribution transformer aging," *Electric Power Systems Research*, 2017, 148, pp. 202 – 209. doi:10.1016/j.epr.2017.03.022
- [18] M. Bazrafshan, and N. Gatsis, "Comprehensive modeling of three-phase distribution systems via the bus admittance matrix," *IEEE Transactions on Power Systems*, 2018, 33, (2), pp. 2015–2029. doi:10.1109/TPWRS.2017.2728618
- [19] M.J.E. Alam, K.M. Muttaqi and D. Sutanto, "A three-phase power flow approach for integrated 3-wire MV and 4-wire multigrounded LV networks with rooftop solar PV," *IEEE Transactions on Power Systems*, 2013, 28, (2), pp. 1728–1737. doi:10.1109/TPWRS.2012.2222940
- [20] S. Arora and B. Barak, "Computational complexity: A modern approach," Cambridge University Press, 2009.
- [21] C. Robert and G. Casella, "Introducing Monte Carlo methods with R," Use R., Springer, 2010.
- [22] M. Abdelaziz, "GPU-OpenCL accelerated probabilistic power flow analysis using Monte-Carlo simulation," *Electric Power Systems Research*, 2017, 147, pp. 70 – 72. doi:10.1016/j.epr.2017.02.022
- [23] K. P. Schneider, B. A. Mather, B. C. Pal, C. . Ten, G. J. Shirek, H. Zhu, J. C. Fuller, J. L. R. Pereira, L. F. Ochoa, L. R. de Araujo, R. C. Dugan, S. Matthias, S. Paudyal, T. E. McDermott, and W. Kersting, "Analytic considerations and design basis for the IEEE distribution test feeders," *IEEE Transactions on Power Systems*, vol. 33, no. 3, pp. 3181–3188, May 2018. doi:10.1109/TPWRS.2017.2760011